

# Hyperbranched Polycoumarates with Photofunctional Multiple Shape Memory\*\*

Si-Qian Wang, Daisaku Kaneko, Maiko Okajima, Katsuaki Yasaki, Seiji Tateyama, and Tatsuo Kaneko\*

Shape-memory polymers (SMPs) are smart materials that memorize temporal shapes and recover their original shape in response to an appropriate external stimuli.<sup>[1]</sup> These materials are of importance for physicochemical and biomaterial research, and have been applied to various fields from biomedical<sup>[2]</sup> to textile materials.<sup>[3]</sup> The most extensively investigated SMPs are thermally functionalized SMPs (TSMPs)<sup>[4]</sup> memorizing double,<sup>[5]</sup> triple,<sup>[6,1b,4b]</sup> and even quadruple shapes.<sup>[7]</sup> The memorization of plural shapes is indispensable for accomplishing tailor-made motility. However, the thermal stimulus is usually applied under a contact control. On the other hand, light can be used as a precise stimulus by adjusting to a suitable wavelength, direction, and intensity, thus allowing it to be controlled rapidly and remotely.<sup>[8]</sup> Using the deformation of these materials, one can directly convert light energy into mechanical energy through photochemistry under ultraviolet<sup>[9]</sup> (UV)-, infrared<sup>[10]</sup> (IR)-, and visible-light<sup>[11]</sup> irradiation or through light-induced heating.<sup>[12]</sup> For example, Lendlein used UV light to facilitate shape-memory effects using a reversible [2+2] photocycloaddition reaction.<sup>[9a]</sup> Such photoinduced SMPs (PSMPs) seem to be promising functional materials for biomedical applications, microfluidic chips, and other miniaturized devices. PSMPs memorizing divers shapes would further expand the range of applications, but have not been reported so far. One of the reasons that restrict SMP development is the cross-linked network, which makes SMPs insoluble and their structural analyses difficult. On the other hand, we observed the mechanical modulus enhancement of densely hyperbranched polymers prepared in the absence of a solvent, presumably because of the hyperbranched chain entanglement occurring during propagation from monomers.

Using such an in-bulk polymerization of multifunctional monomers, we developed densely branched polycoumarate derivatives which showed elasticity upon heating, solubility, and photoreactivity, to generate PSMPs properties with multiple shape memory.

We used the difference in the alcoholic hydroxyl reactivity of the condensation reaction with esters and the addition to conjugated double bonds. 4-hydroxycinnamic acid (4HCA, coumaric acid), which was the simplest phenolic acid with conjugated double bonds and succinic acid for coupling, was used to prepare the symmetric diester monomer BMOPS (Table 1 and compound 3 in Scheme S1 in the Supporting Information). Additionally, 4HCA was one of the most popular molecules<sup>[13]</sup> showing a photoreversible [2+2] cycloaddition under UV irradiation at  $\lambda > 280$  nm to form a photodimer containing a cyclobutane ring cleaved by light irradiation at a wavelength shorter than 250 nm,<sup>[14]</sup> and was a bioavailable metabolite of plants and photosynthetic bacteria.<sup>[15]</sup> The BMOPS was then polymerized in the presence of glycols to create a polymer backbone containing hard cinnamoyl and soft aliphatic moieties. The structural balance control of the hard and soft segments was very important to adjust the softening temperature 10–20 °C higher than the room temperature, which is appropriate for imparting TSMPs properties.

The BMOPS was initially polymerized with 1,2-ethanediol (2C) with conventional catalysts such as  $\text{Na}_2\text{HPO}_4$ ,  $\text{NaH}_2\text{PO}_4$ ,  $\text{KH}_2\text{PO}_4$ ,  $\text{K}_2\text{HPO}_4$ , and  $\text{Al}_2(\text{PO}_4)_3$  for the preparation of polyester poly(BMOPS-co-2C) (poly2C), which only yielded oligomers with molecular weights ( $M_w$ ) of  $3.10 \times 10^3$ ,  $2.25 \times 10^3$ ,  $3.53 \times 10^3$ ,  $2.85 \times 10^3$  and  $3.20 \times 10^3$ , respectively, after three days of polymerization at 200 °C.  $\text{HfCl}_4$  and  $\text{Sc}(\text{OTf})_3$  also showed negative results for polymerization in our system, although they have been reported to generate high molecular weight polyesters.<sup>[16]</sup> On the other hand,  $\text{GeO}_2$  was found to efficiently catalyze the reaction, generating a polymer with a  $M_w$  of  $4.83 \times 10^4$  and a molecular weight distribution  $M_w/M_n = 2.49$ . Thus,  $\text{GeO}_2$  was the most efficient catalyst used here to prepare a series of polyesters through the reaction of BMOPS with various diols (Scheme 1; Table 1).

The resultant polymers featured a linear polyester backbone structure, but FT-IR and  $^1\text{H}$  NMR spectroscopies demonstrated a branching formation. FT-IR spectroscopy indicated that a *trans*-cinnamoyl group was successfully introduced into the polymer backbone. (Figure S1; further details are found in the Supporting Information). Detailed analyses using  $^1\text{H}$  NMR spectroscopy elucidated the precise structure, which has branching points formed by the addition

[\*] Dr. S.-Q. Wang, Dr. M. Okajima, Dr. K. Yasaki, Prof. S. Tateyama, Prof. T. Kaneko  
School of Materials Science  
Advanced Institute of Science and Technology  
1-1Asahidai, Nomi, Ishikawa 923-1292 (Japan)  
E-mail: kaneko@jaist.ac.jp

Prof. D. Kaneko  
Department of Applied Chemistry, Faculty of Engineering  
Kyushu Institute of Technology  
Building No.9, 5F-5, 1-1, Sensui-cho, Tobata-ku  
Kitakyushu-shi, Fukuoka, 804-8550 (Japan)

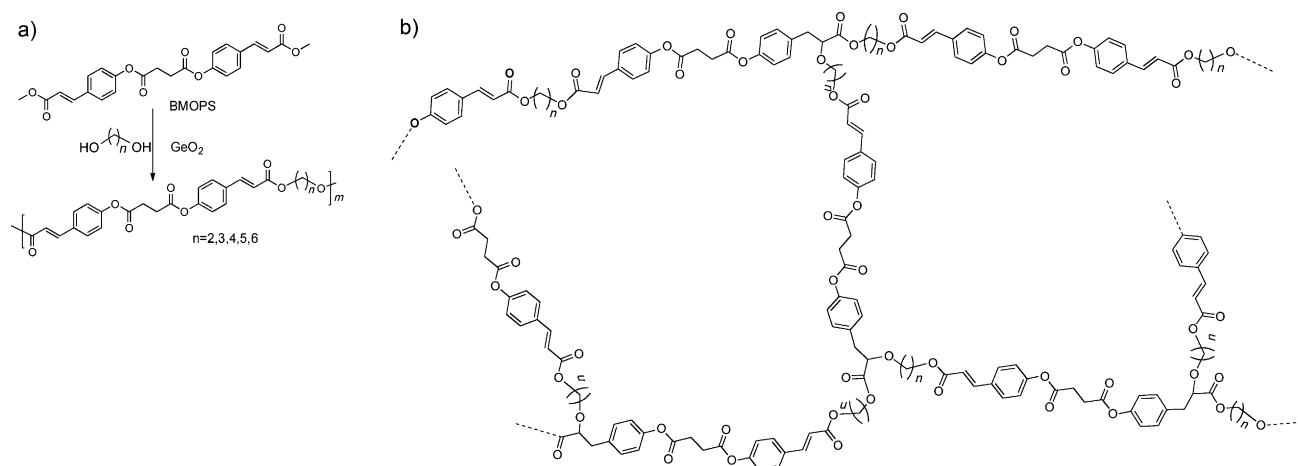
[\*\*] This work was financially supported by Advanced Low Carbon Technology Research and Development Program from Japan Science and Technology Agency (JST-ALCA, grant number 5100270).

Supporting information for this article is available on the WWW under <http://dx.doi.org/10.1002/anie.201305647>.

**Table 1:** Properties of various polyesters (see Scheme 1 for the synthesis).<sup>[a]</sup>

Polymer	BD <sup>[b]</sup>		$M_w$ [g mol <sup>-1</sup> ]	$M_n$ [g mol <sup>-1</sup> ]	$M_w/M_n$	Yield [%] <sup>[c]</sup>	$R_f$ [%] <sup>[e]</sup>	$R_t$ [%] <sup>[e]</sup>
	P	F						
poly2C <sup>[d]</sup>	11.9 (70 h)	29.1 (90 h)	48 300	19 400	2.49	86	93.4	95.2
poly3C <sup>[d]</sup>	13.1 (70 h)	32.3 (90 h)	30 600	13 100	2.34	75	94.2	95.8
poly4C <sup>[d]</sup>	12.5 (70 h)	31.2 (90 h)	30 800	13 500	2.38	83	93.0	95.1
poly5C <sup>[d]</sup>	15.2 (95 h)	42.4 (120 h)	27 400	12 600	2.17	72	92.8	95.7
poly6C <sup>[d]</sup>	12.3 (70 h)	35.2 (90 h)	33 500	23 000	1.95	81	90.6	91.6

[a] Polymerizations of BMOPS (11.4 mmol, 1 equiv) with diols (17.1 mmol, 1.1 equiv) were carried out in the presence of GeO<sub>2</sub> (1 wt%) in a temperature range of 180–220 °C. [b] BD refers to the branching degree. “P” refers to the BD value of polymers processed for SMP, and “F” refers to the BD value of polymers packed together during polymerization. [c] The averaged values from three polymerizations. [d] The polymerization conditions were: 180 °C for 5 h under ambient pressure, 200 °C for 10 h under 1.4 kPa, and 220 °C under 10 Pa until the products became packed together. [e]  $R_f$  and  $R_t$  are averaged values from four times test.  $M_w$  = mass average molecular mass and  $M_n$  = number average molar mass.


**Scheme 1.** a) Syntheses of various polyesters (poly2C, poly3C, poly4C, etc.) obtained from the BMOPS monomer and b) structure of the hyperbranched moiety of the polyesters.

of a hydroxy chain end to the double bond  $-C=C-$  of the cinnamoyl units of the polymer backbone (see Scheme 1). A typical spectrum of poly2C is shown in Figure S2A and S2B. The integral strength ratio of the vinylic protons (2H) to the aromatic ones (4H) should be 0.50 in a theoretically linear polymer structure. The ratio in the present polymer, however, showed a ratio lower than 0.5. Moreover, two sets of new peaks at 3.86–3.97 ppm and 2.98–3.22 ppm were detected. These two new sets of peaks were reasonably assigned to protons in methylene and the methyne of the branching points. The protons from the dimethylene group of the succinate units, marked as **k**, showed multiple signals suggesting the coexistence of a linear coumaryloyl ester and branched coumaryloyl esters. These branched structures occurred in all polymers based on their <sup>1</sup>H NMR findings (Figure S3). Based on these <sup>1</sup>H NMR spectra, the branching degree (BD) was calculated by the integral strength ratio of the vinylic protons to the aromatic ones. Figure S2C showed that the BD increased with polymerization time. Considering the experimental results, the hyperbranched polymer formation process can be divided into two stages. The trifunctional monomer BMOPS had two ester groups and one cinnamic double bond, but the transesterification reaction of the ester group with the hydroxyl group in the presence of GeO<sub>2</sub> catalysis was much more rapid than the hydroxy addition to

the double bond. As a consequence, the linear chains were first propagated by polycondensation of the BMOPS diesters with diols. Most of the end groups of the linear chains should be hydroxyl groups because of the slightly higher ratio of diols than BMOPS in the feed. Next, the hydroxy end reacted to the cinnamic double bond to form branching points. The BD increased as the polymerization time increased; for example, to 11.9% at 70 h in poly2C (Figure S2C) and to 29.1% at 90 h, where the polymer products became rubbery agglomerates and were no longer allowed to agitate. We prepared elastomeric polymers while maintaining their processability by selecting the appropriate polymerization time. As a result, polymers with BD values around 12–15% showed the desired property when the polymerization time was 70 h in poly2C, poly3C, poly4C, and poly6C and 95 h for poly5C, as shown in the 1st column of Table 1. Branching polymer chains are generally not entangled with one another because of steric hindrance of the branch chain ends, and thus their processing is generally difficult. However, the branching polymers prepared without solvents exhibited elastomeric properties above their glass-transition temperatures, but were soluble in solvents such as the trifluoroacetic acid (TFA) /dichloromethane mixture (5/1; Table S1). This phenomenon suggests that the hyperbranched chains were efficiently entangled with one another during chain propagation, to generate physical

cross-linking points. However, they did not form three-dimensional networks, as demonstrated by their good solubility. The sample was easily processed into a film by a hot press at 140 °C and 2 MPa pressure, used for investigating their shape memory behavior.

Thermogravimetric analysis (TGA) showed a decomposition temperature ( $T_d$ ; 10% weight loss temperature) in the range of 319 to 335 °C ( $T_d$  of Figure S4). Differential scanning calorimetry (DSC) showed a glass-transition temperature ( $T_g$ ) from 36 to 64 °C ( $T_g$  of Figure S4). This implied that these materials had  $T_g$ s slightly higher than room temperature, and were appropriate for thermally induced SMP and had  $T_d$ s high enough to use stably. Odd/even effects were clearly observed in the  $T_g$ s and  $T_d$ s, which were probably attributed to a zigzag packing of the polymer chains.<sup>[17]</sup> This thermally controlled SMP behavior was investigated using poly4C as a representative sample, as shown in Figure 1. To quantify a shape-memory effect for all polymers prepared here, the strain fixity rate  $R_f$  as well as the strain recovery rate  $R_r$  were calculated and summarized in Table 1. The  $R_f$  and  $R_r$  values of all prepared polymers were higher than 91% for all cycles, indicating good shape-memory properties in spite of the lack of three-dimensional networks. They started to recover their shape immediately within 15 s when heated again to 60 °C (Figure 1). Other polymers also showed good shape-memory recovery within 25 s when heated to temperature higher than their  $T_g$ s.

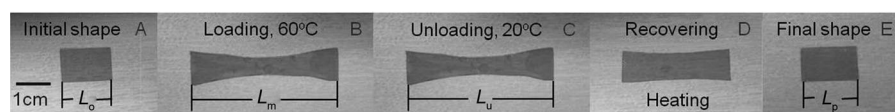


**Figure 1.** Photographs showing the process of shape-memory recovery of the poly4C sample taken with a digital camera. The permanent shape is a film (12 mm × 8 mm × 0.5 mm). When the deformed sample was heated at 60 °C over its  $T_g$  again, it started to recover its shape immediately. The deformed sample recovered to the original shape in 15 s ( $L$  = length).

Next, we investigated their photodeformation capability in the case of poly2C fabricated into a film of 25 mm length, 10 mm width, and 200  $\mu$ m thickness. UV light ( $\lambda$  = 280–450 nm) was exposed to the film from the upper side, and the free edge of the film quickly lifted up to form a concave shape (Figure 2a). However, the films prepared from diols with different methylene groups showed different bending speeds under the same conditions of UV-light irradiation; the speed increased with an increase in the spacer under the same intensity of UV light (Figure 2b). For example, it took 20 s for the poly2C film to complete the photobending with irradiation of UV light at an intensity of 65 mW cm<sup>-2</sup>, while it took only 3 s for poly6C. This phenomenon may be due to the different flexibilities as implied by the different  $T_g$ s. We also found that the bending speed can be controlled by changing the intensity of UV light, and moreover the film bending was not homogeneous upon irradiation by UV light from an oblique direction. Under the most suitable UV-light intensity ( $\lambda$  = 280–450 nm) and a direction, the flat film curled remark-

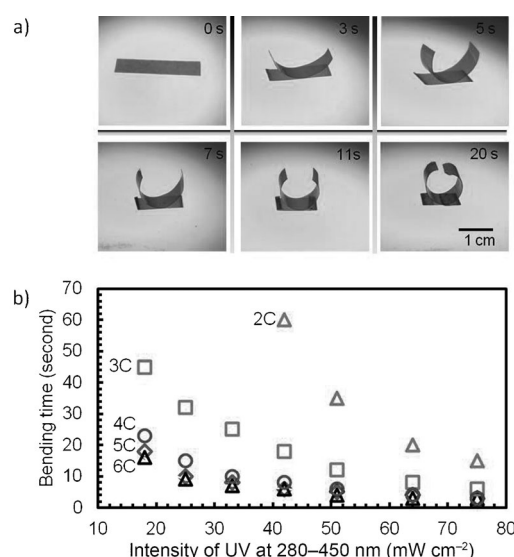


**Figure 2.** a) A series of photographs demonstrating the macroscopic photoinduced bending of a poly2C film (25 mm × 10 mm × 0.2 mm) by UV-light irradiation at  $\lambda$  = 280–450 nm. The final shape remained stable after the light was turned off. b) Bending time versus UV-light intensity in various polymers with different methylene groups in the corresponding glycols. It showed different bending speeds under the same conditions of UV-light irradiation, with the speed clearly increasing with increased carbon chain length from 2C to 4C and keeping a similar speed as 4C, 5C, and 6C. Legends such as 2C, 3C, 4C, 5C, and 6C refer to poly2C, poly3C, poly4C, poly5C, and poly6C, respectively.

ably to a round shape until one edge touched the other edge. The round shape was very stable after the light was turned off. Based on our previous report on a poly(*m*-hydroxycinnamic acid) film,<sup>[13e]</sup> one can easily hypothesize that the present bending behavior could be attributed to the formation of a gradient structure by the photoreaction from the cinnamic

double bonds into cyclobutane as demonstrated by subsequent IR- and UV-light studies.<sup>[9a,b]</sup> As shown in Figure 3, it was observed that the round shape B gradually recovered to the original shape A when low-pressure UV light at  $\lambda$  = 250 nm was used for poly2C, probably because of cyclobutane rings cleaved by such short wavelength UV light. To recover the shape, it took 20–30 minutes for poly6C, poly5C, poly4C, and poly3C, and 3 h for poly2C, presumably because of the high  $T_g$ . From the DSC measurement, it has been proven that poly2C exhibited a higher  $T_g$  than poly3C, poly4C, poly5C, and poly6C, demonstrating that the mobility of the polymer segments in poly2C is lower than that in others; therefore, poly2C bent and recovered more slowly. The photosensitivity from shape A to shape B means that energy transformation from light to mechanical power can be realized instantaneously, which would be widely applicable because it can be controlled remotely just by manipulating the irradiation conditions. The most extensively investigated photoinduced bending properties are based on azobenzene materials.<sup>[18]</sup> In

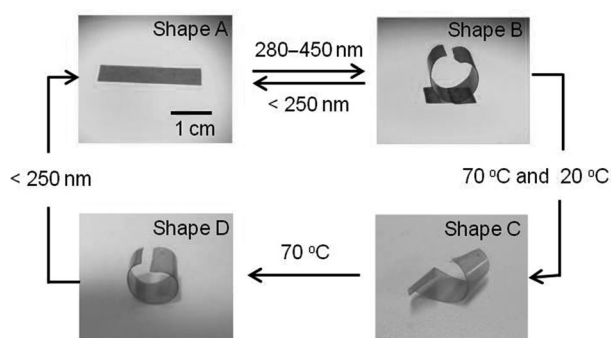


**Figure 3.** Series of photographs of the poly2C sample showing a photo-induced multifunctional shape memory. The permanent shape A was irradiated by UV light at  $\lambda = 280\text{--}450\text{ nm}$  for 20 s to form shape B. Upon being deformed by an external load to the screw shape at  $70\text{ }^{\circ}\text{C}$  and cooled/fixed at room temperature, shape C was fixed. Shape D, which is the same as shape B, was recovered by heating again to  $70\text{ }^{\circ}\text{C}$ . Shape A was recovered by irradiation with a low-pressure Hg lamp at  $\lambda = 250\text{ nm}$  for 180 minutes. The size of shape A is  $25\text{ mm} \times 10\text{ mm} \times 0.2\text{ mm}$ .

contrast, cinnamate polymers as photobending materials with a high speed over the second time range have been rarely reported. The response of our bio-based polymers is much faster than that of the reported azobenzene gels.<sup>[19]</sup> Figure 4a

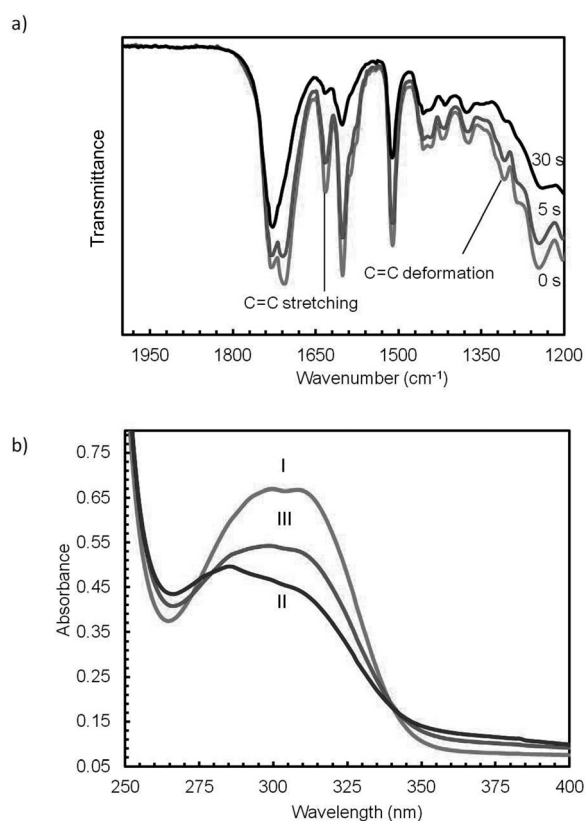


**Figure 4.** a) Changes in the IR spectrum of a poly2C film by UV irradiation. b) UV/Vis absorption spectra of I) the poly2C film, II) which was exposed to a high-pressure Hg-lamp of  $\lambda = 280\text{--}450\text{ nm}$  for 1 minute, followed by III) exposure to a low-pressure Hg-lamp at  $\lambda = 250\text{ nm}$  for 60 minutes.

shows a change in the IR spectrum of a poly-2C film by a high-pressure Hg-lamp with  $\lambda = 280\text{--}450\text{ nm}$ . The absorptions of the *trans* C=C bond at  $1632$  and  $1308\text{ cm}^{-1}$  decreased with increasing irradiation time. The peaks almost disappeared after irradiation for 30 s, suggesting that the cycloaddition of a vinylenic group occurred with the irradiation. The ester carbonyl absorption at  $1705\text{ cm}^{-1}$  decreased with increasing UV-light irradiation time, which was caused by the loss of conjugation with the aromatic group. Although both surfaces of this film were also checked by ATR/IR spectroscopy (ATR = attenuated total reflection), only the irradiated side showed these peak changes, suggesting that these reactions only occurred after irradiation. The UV/Vis spectrum change of the film (Figure 4b) supported the discussion regarding the IR studies. The UV/Vis spectra (I) of the film showed a strong absorbance peak around  $303\text{ nm}$  assigned to the conjugated  $\pi$ -electron bonds of the cinnamoyls. However, the absorbance peak reduced greatly and shifted to around  $285\text{ nm}$  (II) when the film surface was irradiated by a high-pressure Hg lamp for one minute. Upon subsequent exposure to a low-pressure Hg lamp at  $\lambda = 250\text{ nm}$  for 60 minutes, the absorbance peak intensified and shifted back to about  $300\text{ nm}$  (III), supporting a reversible reaction. Thus a photomemorized shape can be well controlled and recovered by changing the irradiation time, direction, and wavelength.

We illustrated here an interesting recovery cycle under light and heat control, and a typical example of poly2C is shown in Figure 3. The mechanically stable, round-shape B was further deformed to a screwed shape by force at  $70\text{ }^{\circ}\text{C}$ , and then cooled to room temperature to fix it as shape C. The screwed shape C can be quickly recovered to a photonically memorized shape (shape D) in about 10 seconds when it was only heated again to over  $70\text{ }^{\circ}\text{C}$ , which is TSMP behavior. When the curled shape B (first memory) was fixed to the screw shape C by force, it caused strain energy to be stored inside, thus forming another memory temporarily (second memory). Here, the chain segment acted like a molecular switch that was depended on the  $T_g$ . Heating above the  $T_g$  made the chain segment become motile and triggered the recovery from shape C to shape D, which is the same as shape B. UV light applied to the film surface causes the creation of a covalently cross-linked structure through photocycloaddition, which increases the effect of maintaining the stable shape (shape B). Thus, the irradiated films showed good recovery. Shape D deformed into the original shape A upon irradiation by UV light at  $\lambda = 250\text{ nm}$  for 3 h. In this process, the shape was additionally controlled by the photo-irradiation time and direction, and the resulting shape was still stable to induce another TSMP. The cycle of shape recovery was well realized and controlled by light and heat. To further expand the potential application the more complex shape-memory ability was explored. The permanent shape of a flying swan was well processed from its ginkgo leaf by repeated UV-light irradiation to both sides (shapes A to B in Figure 5; see Movie SI and Movie SII). Afterward, the temporal shape of a sleeping swan (shape C in Figure 5) was fixed by forcing at  $60\text{ }^{\circ}\text{C}$  and cooling to  $20\text{ }^{\circ}\text{C}$ . The photomemorized shape of a swan was recovered in 60 s from shape C to D by heating again to over  $60\text{ }^{\circ}\text{C}$  (see Movie SIII).



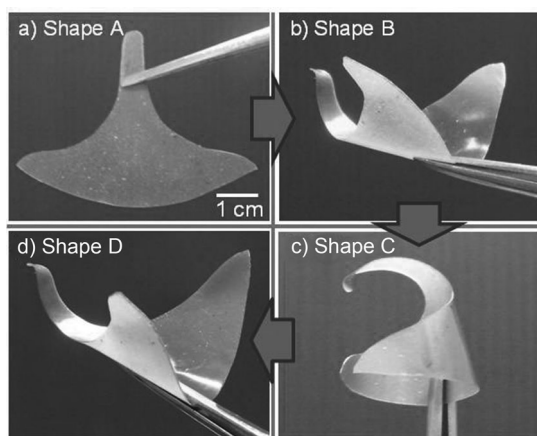


**Figure 5.** A typical complex photoinduced shape-memory effect. a) A poly4C film with a ginkgo leaf shape (shape A) processed by a hot press at 140°C under a pressure of 2 MPa for 30 s. b) The shape of a flying swan (shape B) was processed from shape A by repeating irradiation by UV light at  $\lambda = 280\text{--}450\text{ nm}$  to the desired sides under different conditions. See also Movies SI and SII. c) The shape of a sleeping swan (shape C) was formed at 60°C and was fixed by cooling to 20°C while maintaining the mechanical force. d) The sample with the shape C was put into hot water at 60°C and then the shape of a flying swan (shape D is equal to shape B) was gradually recovered in 60 seconds. See Movie SIII.

The fast recovery of shape B in 13 seconds was observed from the ginkgo leaf shape just by flattening the shape of a flying swan at 60°C and cooling to 20°C. Even when the temporal shape with a large strain, such as the sleeping swan obtained by inversed bending of the wings and neck, was processed, the sample still showed the recovery of the shape of a flying swan. The repeating local deformation to form such a complex shape was realized based on the small UV-light guide with a diameter of 7 mm. A thin optical fiber is expected to work on the formation of a much smaller sculpture. This is a multiple shape memory, realized by the two different stimuli of heat and photoirradiation, and to the best of our knowledge this is the first report on multiple shape-memory materials.

In conclusion, hyperbranched coumarate polyesters were newly synthesized by the polycondensation of BMOPS with various diols. These polymers exhibited elastomeric properties, but good solubility and processability by a hot-press to form films. The film showed both thermal and photoinduced shape-memory effects. The capabilities of these polymers to show a multifunctional shape memory from pre-determined complex temporary shapes and subsequently recover their original shape at ambient temperatures by remote light activation and heating may lead to a variety of potential applications, such as medical and light-driven actuators, in the future.

## Experimental Section

BMOPS was prepared from the starting material of 4HCA reacting with succinyl dichloride. The structure of the BMOPS was characterized by its single crystal (Figure S5). Various polyesters poly-(BMOPS-co-diols) were prepared by the conventional thermal

polycondensation of BMOPS and diols. The detailed experimental procedures and chemical synthesis are described in the Supporting Information.

Received: July 1, 2013

Published online: September 5, 2013

**Keywords:** coumarates · photochemistry · polymers · smart materials

- [1] a) A. Lendlein, V. P. Shastri, *Adv. Mater.* **2010**, *22*, 3344–3347; b) A. Lendlein, S. Kelch, *Angew. Chem.* **2002**, *114*, 2138–2162; *Angew. Chem. Int. Ed.* **2002**, *41*, 2034–2057; c) D. Ratna, D. J. K. Kocsis, *J. Mater. Sci.* **2008**, *43*, 254–269.
- [2] For some examples in the biomedical field, see: a) A. Lendlein, R. Langer, *Science* **2002**, *296*, 1673–1676; b) W. Sokolowski, A. Metcalfe, S. Hayashi, L. Yahia, J. Raymond, *Biomed. Mater.* **2007**, *2*, S23–S27; c) P. R. Buckley, G. H. McKinley, T. S. Wilson, W. Small IV, W. J. Bennett, J. P. Bearinger, M. W. McElfresh, D. J. Maitland, *IEEE Trans. Bio-med. Electron.* **2006**, *53*, 2075–2083.
- [3] a) Q. H. Meng, J. L. Hu, Y. Zhu, J. Lu, Y. Liu, *Smart Mater. Struct.* **2007**, *16*, 1192–1197; b) Q. H. Meng, J. L. Hu, *Composites Part A* **2009**, *40*, 1661–1672.
- [4] For some reviews in this field, see: a) P. T. Mather, X. Luo, I. A. Rousseau, *Annu. Rev. Mater. Res.* **2009**, *39*, 445–471; b) M. Behl, A. Lendlein, *Mater. Today* **2007**, *10*, 20–28; c) M. Behl, M. Yasar, A. Lendlein, *Adv. Mater.* **2010**, *22*, 3388–3410; d) C. Liu, H. Qin, P. T. Mather, *J. Mater. Chem.* **2007**, *17*, 1543–1558.
- [5] a) J. H. Li, J. A. Viveros, M. H. Wrue, M. Anthamatten, *Adv. Mater.* **2007**, *19*, 2851–2855; b) R. A. Weiss, E. Izzo, S. Mandelbaum, *Macromolecules* **2008**, *41*, 2978–2980; c) C. M. Yakacki, N. S. Satarkar, K. Gall, R. Likos, J. Z. Hilt, *J. Appl. Polym. Sci.* **2009**, *112*, 3166–3176; d) S. Han, B. H. Gu, K. H. Nam, S. J. Im, S. C. Kim, S. S. Im, *Polymer* **2007**, *48*, 1830–1834.
- [6] M. Behl, I. Bellin, S. Kelch, W. Wagermaier, A. Lendlein, *Adv. Funct. Mater.* **2009**, *19*, 102–108.
- [7] T. Xie, *Nature* **2010**, *464*, 267–270.
- [8] For some examples of reviews on light stimuli, see: a) V. Balzani, A. Credi, M. Venturi, *Chem. Soc. Rev.* **2009**, *38*, 1542–1550; b) M. M. Russew, S. Hecht, *Adv. Mater.* **2010**, *22*, 3348–3360; c) H. Jiang, S. Kelch, A. Lendlein, *Adv. Mater.* **2006**, *18*, 1471–1475; d) R. J. Wojtecki, M. A. Meador, S. J. Rowan, *Nat. Mater.* **2011**, *10*, 14–27.
- [9] For some examples on UV-induced shape memory, see: a) A. Lendlein, H. Jiang, O. Jünger, R. Langer, *Nature* **2005**, *434*, 879–882; b) L. Wu, C. Jin, X. Sun, *Biomacromolecules* **2011**, *12*, 235–241; c) J. R. Kumpfer, S. J. Rowan, *J. Am. Chem. Soc.* **2011**, *133*, 12866–12874.
- [10] For some examples on IR-induced shape memory, see a) J. Leng, X. Wu, Y. Liu, *J. Appl. Polym. Sci.* **2009**, *114*, 2455–2460; b) H. Koerner, G. Price, N. A. Pearce, M. Alexander, R. A. Vaia, *Nat. Mater.* **2004**, *3*, 115–120.
- [11] Z. H. Hu, B. R. Kanth, R. Tamang, B. Varghese, C. H. Sow, P. K. Mukhopadhyay, *Smart Mater. Struct.* **2012**, *21*, 032003.
- [12] J. Leng, D. Zhang, Y. Liu, K. Yu, X. Lan, *Appl. Phys. Lett.* **2010**, *96*, 111905.
- [13] a) T. Kaneko, H. T. Tran, M. Matsusaki, D. J. Shi, M. Akashi, *Nat. Mater.* **2006**, *5*, 966–970; b) S. Q. Wang, D. Kaneko, K. Kan, X. Jin, T. Kaneko, *Pure Appl. Chem.* **2012**, *84*, 2559–2568; c) M. Chauzar, S. Tateyama, T. Ishikura, K. Matsumoto, D. Kaneko, K. Ebitani, T. Kaneko, *Adv. Funct. Mater.* **2012**, *22*, 3438–3444; d) S. Q. Wang, S. Tateyama, D. Kaneko, S. Ohki, T. Kaneko, *Polym. Degrad. Stab.* **2011**, *96*, 2048–2054; e) K. Yasaki, T. Suzuki, K. Yazawa, D. Kaneko, T. Kaneko, *J. Polym. Sci. Part A* **2011**, *49*, 1112–1118; f) T. Kaneko, D. Kaneko, S. Q. Wang, *Plant Biotechnol.* **2010**, *27*, 243–250.

- [14] M. Nagarathinam, A. M. P. Peedikakkal, J. J. Vittal, *Chem. Commun.* **2008**, 5277–5288.
  - [15] a) N. Ricarda, J. M. Anthony, M. Cathie, *Nat. Biotechnol.* **2004**, 22, 746–754; b) P. Tuan, N. Park, X. H. Li, H. Xu, H. H. Kim, S. Park, *J. Agric. Food Chem.* **2010**, 58, 10911–10917.
  - [16] a) K. Ishihara, S. Ohara, H. Yamamoto, *Science* **2000**, 290, 1140–1142; b) A. Takasu, Y. Lio, Y. Oishi, Y. Narukawa, T. Hirabayashi, *Macromolecules* **2005**, 38, 1048–1050.
  - [17] L. J. Francisca Mary, P. Kanan, *J. Polym. Sci. Part A* **1999**, 37, 1755–1761.
  - [18] Y. Zhao, T. Ikeda in *Smart Light-Responsive Materials*, Wiley, New Jersey, **2009**.
  - [19] a) Y. L. Yu, M. Nakano, A. Shishido, T. Shiono, T. Ikeda, *Chem. Mater.* **2004**, 16, 1637–1643; b) H. Finkelmann, E. Nishikawa, G. G. Pereira, M. Warner, *Phys. Rev. Lett.* **2001**, 87, 015501.
-